ELSEVIER

Catalysis Today 26 (1995) 267–274

CATALYSIS TODAY

Numerical simulation of the two-dimensional flow in high pressure catalytic combustor for gas turbine

Y. Tsujikawa [a,*], S. Fujii [a], H. Sadamori [b], S. Ito [b], S. Katsura [c]

[a] *Department of Aerospace Engineering, University of Osaka Prefecture, 1-1 Gakuen-cho, Sakai 593, Japan*

[b] *Research and Development Center, Osaka Gas Company, 19-9, 6-chome Torishima, Konohana-Ku, Osaka 554, Japan*

[c] *Nanko R and D Laboratory, Osaka Gas Information System Research Institute, 8-12-2 Nanko-higashi, Suminoe-Ku, Osaka 559, Japan*

Abstract

The objective of this paper is modeling the mechanism of high pressure and high temperature catalytic oxidation of natural gas, or methane. The model is two-dimensional steady-state, and includes axial and radial convection and diffusion of mass, momentum and energy, as well as homogeneous (gas phase) and heterogeneous (gas surface) single step irreversible chemical reactions within a catalyst channel. Experimental investigations were also made of natural gas, or methane combustion in the presence of Mn-substituted hexaaluminate catalysts. Axial profiles of catalyst wall temperature, and gas temperature and gas composition for a range of gas turbine combustor operating conditions have been obtained for comparison with and development of a computer model of catalytic combustion. Numerical calculation results for atmospheric pressure agree well with experimental data. The calculations have been extended for high pressure (10 atm) operating conditions of gas turbine.

Keywords: Combustion; Numerical simulation; Gas turbine; Two-dimensional flow

1. Introduction

The concept of catalytic combustion has received increasing attention in these days due to its potential for reducing pollutant emissions, most notably oxides of nitrogen (NO_x) accompanied by extended lean limits when operating at high combustor inlet velocities [1,2]. It enables realization of the uniform temperature distribution and stable combustion. Therefore, the technology can be applied to the gas turbine combustor. Implementation of catalytic combustion concepts in gas turbine engine technology has been the goal of much recent research, for which reduced emissions is the motivation. Kajita et al. [3] have found the obvious signs of catalyst deactivation, and recommended that the future research on gas turbine catalytic combustion be concentrated in the area of extending catalyst life.

In a conventional gas turbine combustor, the temperature rise from 450 to 1 100°C is required, so that only one kind of catalyst could not cover this wide temperature range. The catalyst with high temperature activity, in addition to that at rather low temperature, has been under development [4]. Griffin et al. have also done experimental work where they have demonstrated that the inclusion of active catalytic surfaces can serve to provide heat and reactive intermediates to the nearby gas phase thereby improving local fuel mixing due to reaction in a boundary layer [5]. Use of catalysts in hybrid gas turbine applications,

* Corresponding author.

SSDI 0920-5861(95)00148-4

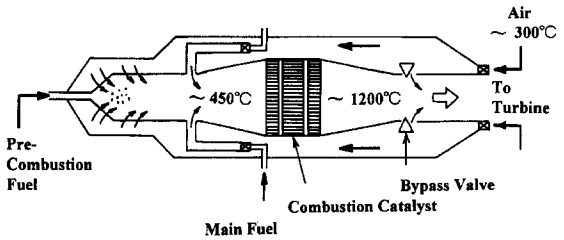

Fig. 1. Schematic construction of the catalytic combustor.

Stage	Catalyst
A	Noble Metal Catalysts
B	
C	
D	Mn-Substituted Hexaaluminate Catalysts
E	
F	
G	

Fig. 2. The combustion catalyst system.

Table 1
The goal of our catalytic combustor for gas turbine

Item	Target
Applied turbine	
Capacity	1 000, 1 500 kW
Max. inlet temp.	1 100°C
Pressure	10 atm, abs
NO_x emissions	40 ppm (0% O_2)
Combustion efficiency	>99%
Pressure loss ratio	<5%
Catalyst life	8 000 h, 400 cycles
Fuel	Natural Gas

which consists of a homogeneous combustion zone followed by a catalytic combustion zone, may provide a more near-term approach to the use of catalytic combustion in commercial applications when compared to conventional monolith designs [6,7]. In the present study, we adopted the multi-stage catalytic combustor as a simulation model. The temperature distribution, fuel concentration and the fraction of surface reaction to the homogeneous reaction can be made clear and compared with those obtained from experimental work.

2. Numerical simulation

The details of the flow within the catalyst channel can be very important for optimum combustor design. The monolith channel is very small, so that the experimental analysis to obtain the characteristics of the flow within it is very difficult. So far the initial and final conditions are known, but the processes that bring about the changes are unclear, the so-called 'black box' [8].

2.1. Model description (experimental apparatus)

In a catalytic gas turbine combustor, the preheated air and natural gas are premixed in advance. The schematic construction of the experimental combustor is shown in Fig. 1. The characteristic of the combustor is that the combustion occurs within the honeycomb-shaped combustion catalyst layer. It consists of seven catalyst stages, denoted as A to G. Each axial length of flow passage is 20 mm as shown in Fig. 2. The noble metal catalysts are used in stage A to C, and Mn-substituted hexaaluminate catalysts in stage D to G. These are classified into high temperature activated and low temperature type. The goal of the catalytic combustor for gas turbine engine is proposed by one of authors as shown in Table 1 [9]. The calculation is executed for monolith channels of the stage D to G. The details of the flow within the monolith is shown in Fig. 3 [10]. This study was undertaken to help to elucidate the detailed fluid mechanics of flows within catalytic monoliths. Improved understanding will assist in the optimization of design procedure of combustion catalysts.

2.2. Computational procedure

The catalyst wall temperature strongly affects the catalytic life, which is important in the design of a monolithic combustor for gas turbine application. So far, only a one-dimensional well mixed plug flow model has been extensively used and the reactions solved for are either first order or

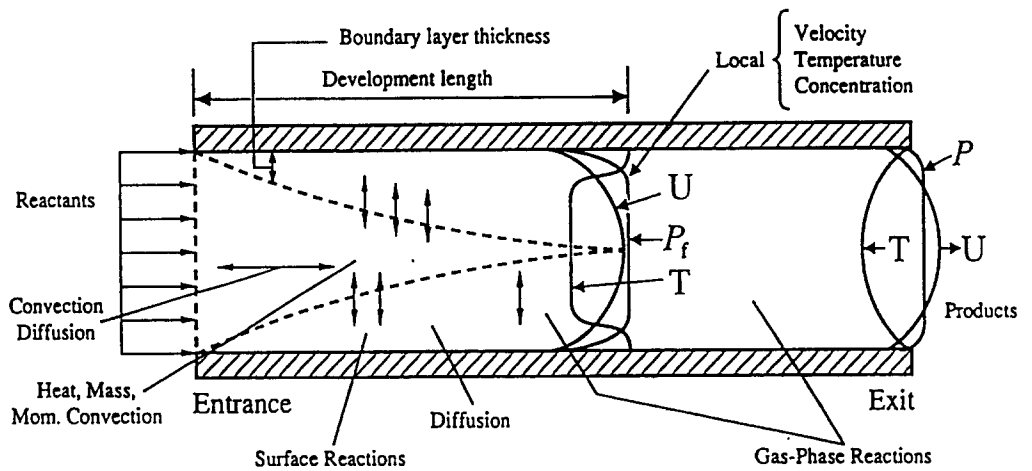

Fig. 3. Flow within the catalyst monolith channel (Adapted from Bracco [10]).

mass transfer controlled [11,12]. However, these models introduce difficulty due to the numerical stiffness. In the present study, the flow is assumed to be two-dimensional axisymmetric. The continuity, momentum and energy equations have been solved simultaneously. Further, some chemical reactions must be included. All the dependent variables of interest here obey a generalized conservation principle. If the dependent variable is denoted by ϕ, the generalized two-dimensional axisymmetric differential equation is

$$r\frac{\partial\phi}{\partial t}+\frac{\partial}{\partial x}\left\{r\left(u\phi-\Gamma\frac{\partial\phi}{\partial x}\right)\right\}+\frac{\partial}{\partial r}\left\{r\left(v\phi-\Gamma\frac{\partial\phi}{\partial r}\right)\right\}=S \quad (1)$$

where Γ is the diffusion coefficient, and S is the source term. These values for each dependent variables are listed in Table 2.

The real difficulty in the calculation of the velocity field lies in the unknown pressure field. The pressure field is indirectly specified via the continuity equation. When the correct pressure field is substituted into the momentum equations, the resulting velocity field satisfies the continuity equation. Such a procedure is given the name SIMPLE (semi-implicit method for pressure-linked equations) [13]. Computational domain is bounded between catalyst wall and inlet and outlet sections. Fig. 4 shows the physical computational domain (17×17). In addition, we recognize that we should not calculate all the variables for the same grid points. The displaced or 'staggered' grid are used in the present study (Fig. 5).

The simplified model is made up with the following assumptions as;

(1) The flow in monolith channel is incompressible and laminar.

(2) At the catalyst surface, the flow is adiabatic and satisfies no-slip condition.

(3) The characteristics of catalyst are measured by the conventional micro-reactor test with 0.5% fuel-air mixture using crushed catalytic material, the data obtained can be used extensively to high temperature region. Fig. 6 shows the Arrhenius plot of Mn-hexaaluminate catalyst for different pressures expected in gas turbine operation (for temperature of 1 200°C). These data have been obtained for the very first time and are considerably valuable. In connection with this figure, the methane complete oxidation rate over Mn-hexaaluminate catalysts is shown by the following equations for the reaction temperature of 1 200 and 1 300°C.

$$r=6.75\times10^{-3}p^{0.8}w_m^{0.8}\exp\left(-\frac{96\,600}{R_0T}\right) \quad (2)$$

for 1 200°C [mol m^{-3} s^{-1}]

$$r=2.0\times10^{-3}p^{0.95}w_m^{0.95}\exp\left(-\frac{96\,400}{R_0T}\right) \quad (3)$$

Table 2
The list of diffusive coefficients and source terms for each dependent variable

ϕ	Γ	S
u	$\nu+\nu_t$	$-r\frac{\partial p}{\partial x}+\frac{\partial}{\partial x}\left(r\Gamma\frac{\partial u}{\partial x}\right)+\frac{\partial}{\partial r}\left(r\Gamma\frac{\partial \nu}{\partial x}\right)$
ν	$\nu+\nu_t$	$-r\frac{\partial p}{\partial r}+\frac{\partial}{\partial x}\left(r\Gamma\frac{\partial u}{\partial r}\right)+\frac{\partial}{\partial r}\left(r\Gamma\frac{\partial \nu}{\partial r}\right)$
T	$\frac{\nu}{\mathrm{Pr}}+\frac{\nu_t}{\mathrm{Pr}_t}$	$-r(-\Delta h)A_h\exp\left(-\frac{E_{ah}}{R_0T}\right)C_f^nC_{O_2}^m p^{n+m}$ or $-r(-\Delta h)A_c\exp\left(-\frac{E_{ac}}{R_0T}\right)C_f^l p^l$
C_f	$\frac{\nu+\nu_t}{D_f}$	$-rA_h\exp\left(-\frac{E_{ah}}{R_0T}\right)C_f^nC_{O_2}^m p^{n+m}$ or $-rA_c\exp\left(-\frac{E_{ac}}{R_0T}\right)C_f^l p^l$
C_{O_2}	$\frac{\nu+\nu_t}{D_{O_2}}$	$-rA_h\exp\left(-\frac{E_{ah}}{R_0T}\right)C_f^nC_{O_2}^m p^{n+m}$

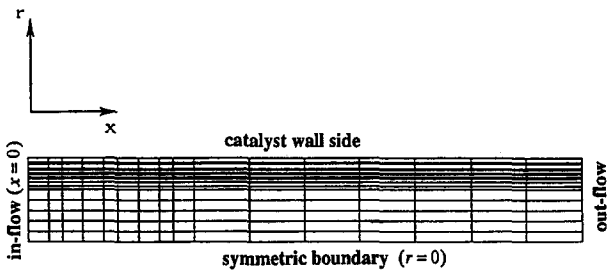

Fig. 4. The computational domain.

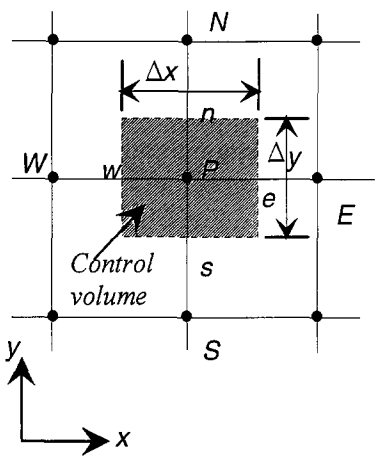

Fig. 5. The Control volume for the two-dimensional situation.

for 1 300°C [mol m^{-3} s^{-1}], where the size of the crushed catalyst particles ranged from 10 to 16 mesh, the methane concentration is 0.5% and space velocity ranged from 6×10^5 to 1.67×10^6 h^{-1}.

(4) The characteristics of the postinduction reaction of methane-oxygen mixtures as studied by Dryer and Glassman [14] encourage speculation that the rate of hydrocarbon reaction can be expressed by a simple global expression of the form of $CH_4+2O_2\rightarrow CO_2+2H_2O$. The rate of reaction in the postinduction phase of the lean methane oxidation in a flow reactor was found to be described well by the overall expression. The gas phase global reaction rate of methane (values of activation energy and preexponential factor) including the influence of pressure is given by the following Eq.

$$r=10^{19.2}\left(\frac{P}{1.013\times10^5\times82.06T}\right)^{1.5}\exp\left(-\frac{48\,400}{1.987T}\right)w_m^{0.7}w_o^{0.8} \quad (4)$$

[mol m^{-3} s^{-1}]

However, it should be noted that the parameters of this equation are significantly different from those found by investigators who have studied the

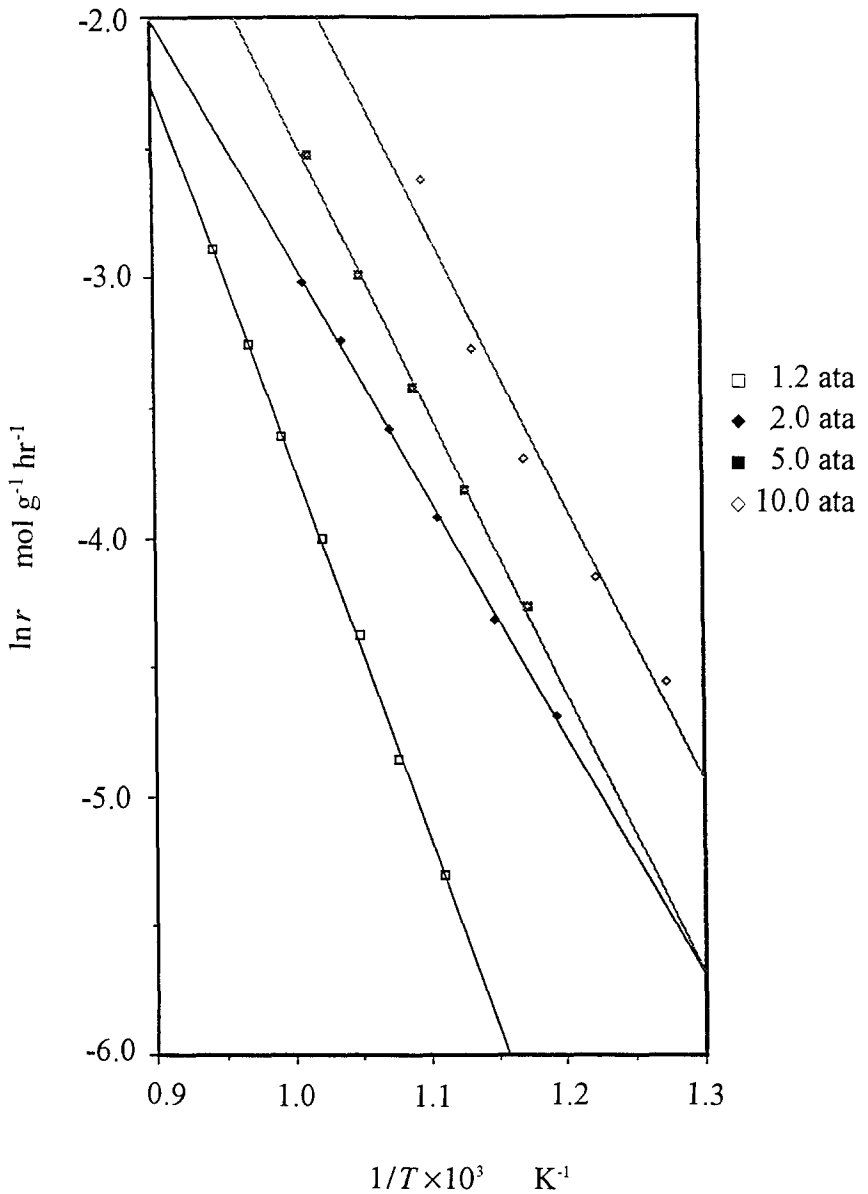

Fig. 6. Arrhenius plot of the Mn-hexaaluminate catalyst. (Effect of pressure.)

induction (ignition delay) phase of their reaction in shock tubes and flow reactors.

3. Results and discussion

In gas turbine application, the natural gas is used as fuel. As mentioned before, only one-step global reaction scheme of pure methane has been included into calculation code. In the experiment, the initial temperature, pressure, the adiabatic temperature and velocity of the mixture at noble metal catalysts stage A, are 450°C, 1.013 MPa, 1 200°C and 3.4 m/s, respectively. However, we could not obtain the characteristics of the noble metal catalysts stage, A to C, accurately, so that we omit these stages from computation. We used the channel inlet temperature of 755°C and residual fuel of 59% as initial conditions for stage D to G. The discussions below are limited to high pressure operating condition of 10 atm. The axial profiles of gas temperature at stage D are shown in

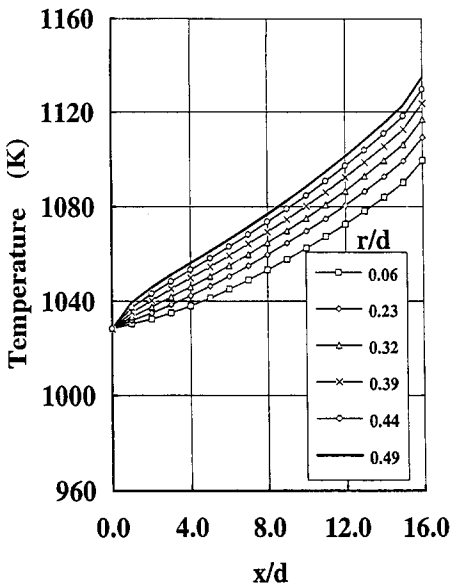

Fig. 7. The axial temperature profiles of stage D.

Fuel concentration: 1.936 %
Linear velocity: 3.4 m/s
Pressure: 10 atm

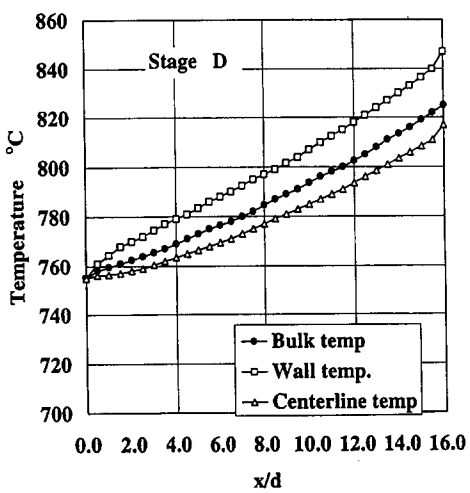

Fig. 8. The temperature profiles of the catalyst wall, the bulk gas and the centerline of stage D.

Fig. 7. Both axial and radial distance are normalized by the hydraulic diameter of catalyst channel, d. The bold solid line ($r/d=0.49$) simulates the catalyst surface temperature. In the present computation, we could not include the properties of catalyst materials, such as thermal conductivity. The most outer control volume is able to simulate the catalyst wall. Under the ambient pressure condition, the catalyst wall temperatures by computation agree very well with those obtained from the experiment using measuring technique with fine thermo-couples inserted into the catalyst channel.

The temperature profiles of catalyst wall, bulk gas and centerline of stage D are depicted in Fig. 8. The bulk gas temperature is raised almost linearly and less than catalytic wall temperature by 20 to 30°C. As the radiative heat transfer at both sides of catalyst channel are not taken into consideration, the temperature drop at the channel exit could not be found.

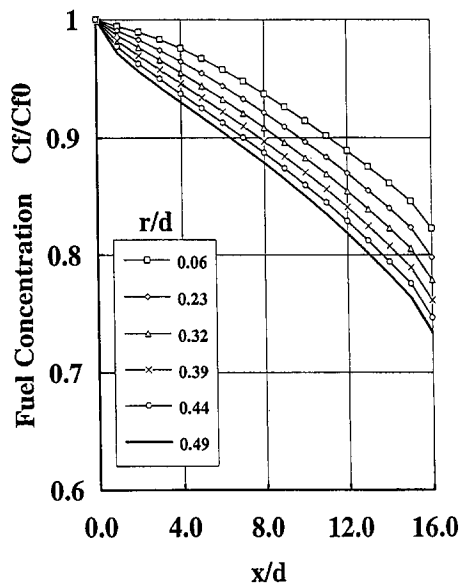

Fig. 9. The axial fuel concentration profiles of stage D.

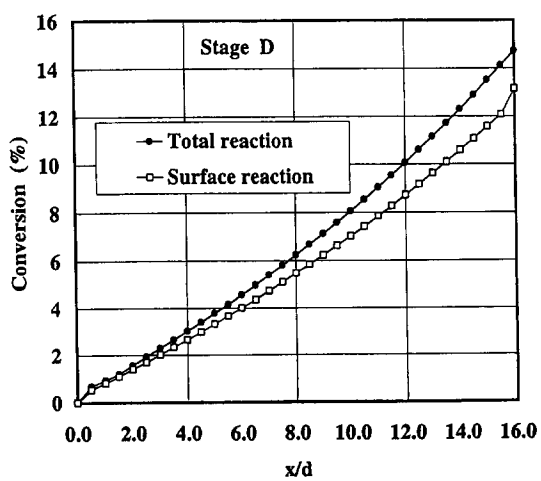

Fig. 10. The contribution of the surface reaction of stage D.

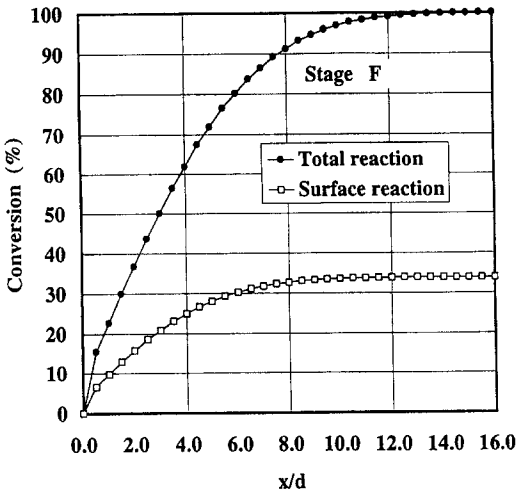

Fig. 11. The contribution of the surface reaction of stage F.

The normalized fuel concentration is shown in Fig. 9. It is clear that the converted fuel fraction is large near the catalyst wall, hence at the stage D the phenomenon can be regarded as diffusion controlled.

Fig. 10 shows the contribution of surface reaction prevailing in total fuel conversion. In stage D, the bulk gas temperature is about 800°C, and at this level of temperature, gas phase reaction is considered to be slight, so we can recognize the no ignition of gas phase reaction occurs. While, in stage F, the bulk gas temperature exceeds 1 100°C, the gas phase reaction is activated considerably, almost 70% of total fuel conversion is due to the homogeneous reactions as shown in Fig. 11.

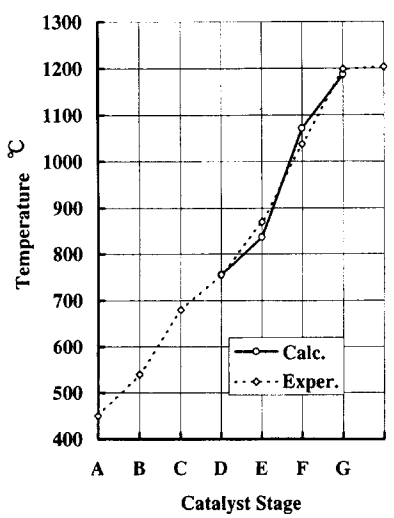

Fig. 12. Comparison between the calculated bulk gas temperature using the present model and the experimental results.

A comparison of the model with experimental catalytic reaction data of actual combustion catalyst for gas turbine was made, demonstrating excellent agreement as shown in Fig. 12. The solid curve showed the bulk gas temperature at exit of each catalyst stages, was obtained from our computer solutions using physical input data corresponding to the experimental operating conditions. Thus actual values for reference velocity, pressure, fuel to air ratio, catalyst length, channel diameter were input parameters, in which the adiabatic temperature is equivalent to that with pure methane.

4. Nomenclature

A_c: preexponential for surface reaction m/s
A_h: preexponential for gas reaction mol/m^{3}s
C_f: fuel concentration mol/m^3
C_{O_2}: oxygen concentration mol/m^3
D: diffusion coefficient m^2/s
d: hydraulic diameter of catalyst channel m
E_{ac}: activation energy for surface reaction J/mol
E_{ah}: activation energy for gas reaction J/mol
Δh: heating value J/mol
p: pressure Pa
Pr: Prandtl number
R_0: universal gas constant J/mol K
r: radius or reaction rate constant m or mol/m^{3}s
S: source term in Eq. (1)
T: temperature K
U, u: axial velocity
W_m: methane mole fraction
W_O: oxygen mole fraction
x: axial flow length m

Greek symbols

ϕ: dependent variable
ν: kinetic viscosity m^2/s
Γ: diffusion coefficient

5. Summary

The two-dimensional axisymmetric CFD code has been developed and applied to the catalytic combustor with high temperature Mn-substituted hexaaluminate catalyst. Even at high pressure condition of 1.013 MPa, which is typical in gas turbine application, the bulk gas temperature and total and/or local fuel conversion can be simulated sufficiently. The contribution of surface reaction in total fuel conversion, in addition, the ignition of homogeneous reaction can be made clear. When the model is used to examine conversion as a function of gas inlet temperature, pressure and fuel to air ratio for typical lean operating conditions with a Mn-substituted hexaaluminate catalyst, a catalytic light-off temperature and the onset of gas phase combustion can be predicted. Therefore, we can conclude that this code is found to be applicable to optimization of the catalytic combustor.

References

[1] W.C. Pfefferle, J. Energy, 2 (1978) 142.
[2] A.E. Cerkanowicz et al., ASME Paper No. 77-GT-85 (1977).
[3] S. Kajita, Y. Tanaka and J. Kitajima, ASME Paper No. 90-GT-89 (1990).
[4] H. Sadamori et al., Proc. 10th Symp. Catal. Combust., 20 (1990) (In Japanese).
[5] T. Griffin et al., Comb. Sci. Tech., 19, 37 (1989).
[6] L.D. Pfefferle., Proc. 2nd Int. Workshop Catal. Combust., Tokyo, 68 (1994).
[7] V.J. Siminsky and H. Shaw, AFAPL-TR-76-80 (1976).
[8] G.C. Wilson, M.F. Bardon and J.J. Witton, ASME Paper No. 92-GT-118 (1992).
[9] H. Sadamori et al., Proc. 2nd Int. Workshop Catal. Combust., Tokyo, 158 (1994).
[10] F.V. Bracco et al., DOE/MC/1406-T1 (1980).
[11] Yoshine et al., Proc. of 18th CIMAC, (1989) 210.
[12] J. Votruba et al., Chem. Eng. Sci., 30 (1975) 117.
[13] S.V. Patankar, Numerical Heat Transfer and Fluid Flow, Hemisphere Publishing, 1980.
[14] F.L. Dryer and I. Glassman, 14th Int. Symp. on Combust, (1973) 987.